

Chapter 13

Nucleotide Excision Repair from Bacteria to Humans: Structure–Function Studies

Ye Peng, Hong Wang, Lucas Santana-Santos, Caroline Kisker,
and Bennett Van Houten

Abstract This chapter describes our present knowledge of nucleotide excision repair (NER) in both prokaryotic and eukaryotic organisms. NER is a generalized repair system capable of removing a wide range of DNA lesions differing in their shape and chemistry. Advances in the structure–function of the proteins that mediate this repair process have given a rich understanding of the key molecular steps that include the following: damage detection, damage verification, incision, repair synthesis, and ligation. The first section of this chapter examines prokaryotic NER, which is mediated by six proteins. The same process in eukaryotic cells requires over 30 proteins, which is covered in the next section. The chapter ends with a brief description of several human diseases that are caused by the loss of NER protein activity.

1 Introduction

One of the most common and versatile DNA repair systems across all forms of life is nucleotide excision repair. This generalized repair system is capable of removing a wide variety of DNA lesions that differ dramatically in their structures and chemical makeup. Several of these substrates are highlighted in Fig. 1. These include UV-induced photoproducts, lesions resulting from anticancer agents such as cisplatin, bulky adducts resulting from attack of activated polycyclic aromatic hydrocarbons (see Chap. 9), and even certain forms of oxidative lesions (see Chap. 10). NER can be described in six interconnected steps, Fig. 2: (1) initial *damage detection* in which the lesion is first marked by a protein, (2) *damage verification* in which a

B. Van Houten (✉)

Department of Pharmacology and Chemical Biology,
University of Pittsburgh School of Medicine, Pittsburgh, PA 15213, USA
and

University of Pittsburgh Cancer Institute, Hillman Cancer Center, University of Pittsburgh,
Pittsburgh, PA 15213, USA

e-mail: vanhoutenb@upmc.edu

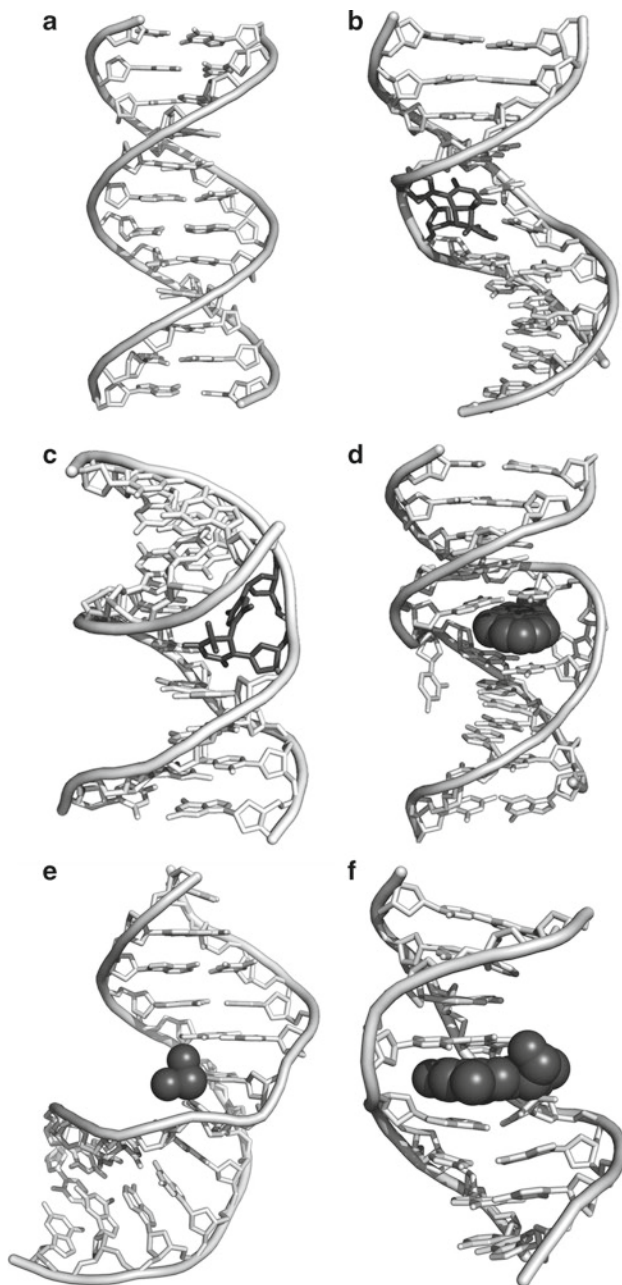


Fig. 1 Nucleotide excision repair (NER) has a vast substrate repertoire. NER can repair damage caused by a variety of sources that cause distortions in the DNA helix and differ dramatically in their chemical structure. (a) Lesion-free B-Form DNA. (b) *cis-syn*-cyclobutane thymine–thymine dimer (CPD) (PDB ID: 1PIB), (c) 6-4 photoproduct (6-4PP) (PDB ID:1CFL), (d) intercalation-based displacement model of 5'^Cmethyl-BPDE-(-*trans*)-N2-deoxyguanine adduct (PDB ID: 1Y9H), (e) cisplatin-1,2-d(guanine–guanine) intrastrand cross-link (PDB ID: 2NPW) and (f) furanoside 4'-hydroxymethyl-4,5',8-trimethylpsoralen-thymine monoadduct (PDB ID: 203D)

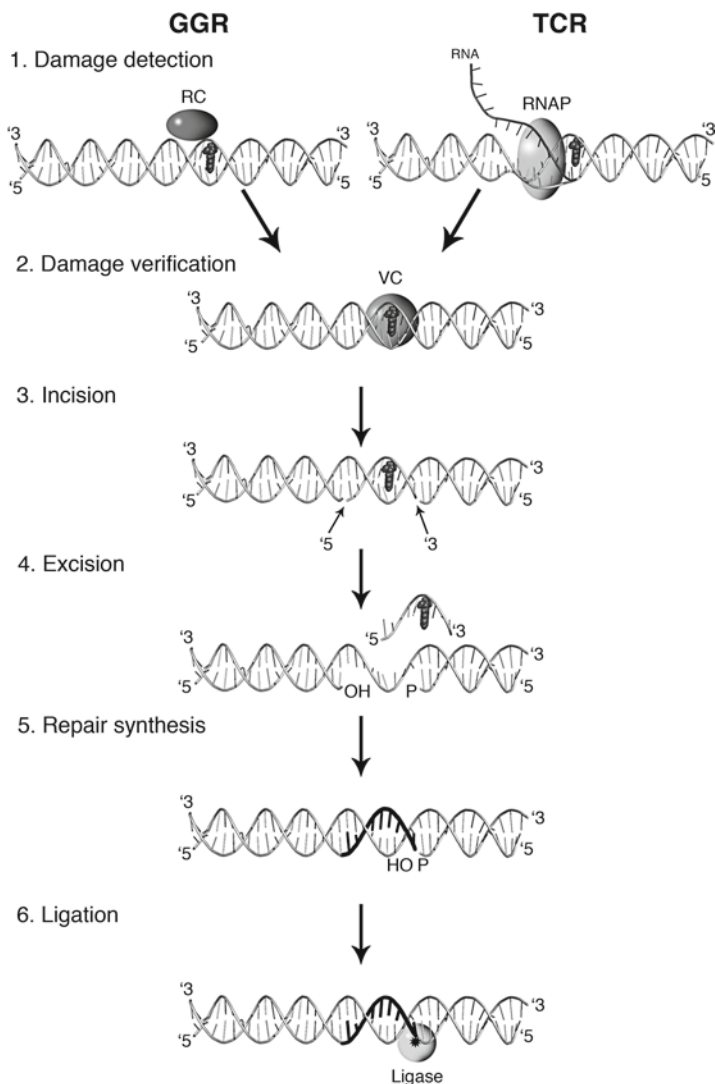


Fig. 2 General model of nucleotide excision repair (NER). NER can be described in six discrete steps. During the first step, damage recognition is achieved either through global genome repair, GGR, (*left*) in which a damage recognition complex (RC) first identifies a damage-induced distortion. The transcription-coupled repair pathway, TCR, is initiated by the stalling of RNA polymerase (RNAP) at the site of damage. The subsequent steps of NER are the same in both pathways, which include the binding of a damage verification complex (VC) (step 2), followed by the recruitment of incision nucleases (step 3) which hydrolyze the phosphate backbone 5' and 3' to the damaged site. In prokaryotes, this incision site occur 4–5 nucleotides 3' and the eight nucleotides 5' to the damaged site, resulting in the release of an oligonucleotide excision product containing the damage of 11–12 nucleotides. In mammalian cells, the 3' incision is at the same position, but the 5' incision is with 15–24 nucleotides considerable further away from the damaged site, such that the dual incisions release a 24–32 oligonucleotide during the excision (step 4). The resulting gap is filled in by DNA polymerase (step 5) and sealed by DNA ligase (step 6)

second protein or protein complex authenticates the presence of a damaged nucleotide, (3) Dual-strand *incision* in which the phosphate backbone is hydrolyzed in two places on the same strand several nucleotides away from the damaged site, (4) *excision* of the lesion and surrounding nucleotides, (5) *repair synthesis* in which replication of one strand is performed to fill in the gap left by the removal of the oligonucleotide containing the damage, and (6) *DNA ligation* in which the newly synthesized repair patch is sealed. Two different subpathways of NER have been characterized and are dependent upon the initial recognition step (Fig. 2). Global genome repair (GGR) is initiated by damage-specific proteins, which dynamically scan vast quantities of DNA, probing for structural perturbations. Transcription-coupled repair (TCR) is initiated by the blockage of RNA polymerase (RNAP) at a damaged site. This stalled RNAP is a signal for the repair enzymes to initiate damage verification and incision. The subsequent steps of NER in both repair pathways are the same. This chapter compares and contrasts NER processes in prokaryotic and eukaryotic cells. Structure–function studies provide a rich and detailed understanding of how these NER proteins function to remove a vast array of DNA lesions.

2 NER in Prokaryotic Cells

Bacterial nucleotide excision repair (NER) was first discovered in the 1960s when Setlow and Carrier (1964) and Boyce and Howard-Flanders (1964) showed that ultraviolet light (UV)-induced thymine cyclobutane dimers (CPD) (Fig. 1b) were actively removed from genomic DNA of *Escherichia coli* strain K-12, but not from a UV-sensitive mutant strain. They proposed a general scheme for the removal of thymine dimers: (1) the photoproducts and surrounding nucleotides were excised from one strand of the DNA; (2) a repair patch was synthesized through complementary base-pairing with the intact opposite strand; and (3) the phosphodiester bonds were rejoined (Boyce and Howard-Flanders 1964). The replication repair step was further characterized by Hanawalt and Haynes (1965), who suggested that the substrate specificity of the NER systems included a large number of chemically distinct lesions.

Hill (1958) and later Howard-Flanders et al. (1966) isolated bacteria that were sensitive to killing by UV and subsequently mapped three loci: *uvrA*, *uvrB*, and *uvrC*. Molecular cloning and overexpression of the products of these three *E. coli* genes by Sancar and Rupp (1983) indicated that these three proteins were both necessary and sufficient for damage recognition and incision. Further biochemical analysis indicated that UvrA initiates repair by recognizing the damage-induced distortion (Mazur and Grossman 1991; Van Houten and Snowden 1993) and then transfers the DNA to UvrB for damage verification (Orren and Sancar 1990; DellaVecchia et al. 2004). The stable UvrB–DNA preincision complex recruits UvrC, an endonuclease that hydrolyzes one phosphodiester bond 4–5 nucleotides 3' and another eight nucleotides 5' to the damaged nucleotide (Sancar and Rupp 1983). UvrD (DNA helicase II), in conjunction with DNA polymerase I, releases the oligonucleotide (Caron et al. 1985; Husain et al. 1985) containing the

Table 1 Nucleotide excision repair proteins in *E. coli*

<i>Escherichia coli</i>			
Name	Amino acids	Molecular weight (kDa)	Function
UvrA	940	103.85	Initial DNA damage recognition
UvrB	673	76.19	DNA damage verification
UvrC	610	68.16	3' and 5' incision nuclease
UvrD	720	82.12	UvrB/UvrC turnover
Mfd	1148	129.88	Transcription-coupled repair
LigI	671	73.65	DNA ligase
PolI	928	103.07	DNA polymerase

damage. DNA polymerase I fills the excised region, and the resulting nick is sealed by DNA ligase I (Caron et al. 1985; Husain et al. 1985). The components involved in prokaryotic NER are summarized in Table 1.

The genomic sequences of over 200 different bacterial species and subsequent alignment of their Uvr proteins have revealed highly conserved residues, suggesting a common NER mechanism in all prokaryotes. This information, in conjunction with biochemical studies from a number of groups combined with the determination of the three-dimensional protein structures through X-ray crystallography and NMR, has allowed a detailed understanding of how these proteins ensure damage recognition and subsequently remove the damaged nucleotides.

2.1 Damage Recognition: UvrA

UvrA functions as damage detector and initiates the NER process. Under physiological conditions, UvrA forms a dimer with a total molecular weight of ~210 kDa (Myles and Sancar 1991). Sequence homology analysis reveals that UvrA belongs to the ATP-binding cassette (ABC) superfamily of ATPases, which couple ATP hydrolysis to diverse cellular functions (Doolittle et al. 1986), Fig. 3a. The ABC ATPase domain shares several common nucleotide-binding motifs among the superfamily: a Walker A motif and a Q loop for nucleotide-binding domain I (NBDI), a Walker B, a signature sequence (Leu-Ser-Gly-Gly), and a His-loop in the second nucleotide-binding domain (NBDII). Each UvrA possesses two ABC modules, and the dimeric UvrA theoretically contains four nucleotide-binding sites (Gorbalenya and Koonin 1990). The structure of the *Bacillus stearothermophilus* UvrA dimer has been recently solved (PDB ID: 2R6F) and demonstrates that all four nucleotide-binding sites are formed in an intramolecular fashion (Pakotiprapha et al. 2008) (Fig. 3a). In addition to the ABC ATPase domain, the structure also reveals that three zinc atoms are coordinated to each UvrA monomer, a situation not found in other ABC ATPases. The third zinc-binding module is thought to interact with DNA to facilitate the recognition specificity for the damage (Croteau et al. 2006; Truglio et al. 2006).

UvrA can hydrolyze both ATP and GTP, and the ATPase/GTPase activity is essential for UvrA to recognize damaged DNA (Van Houten et al. 1988).

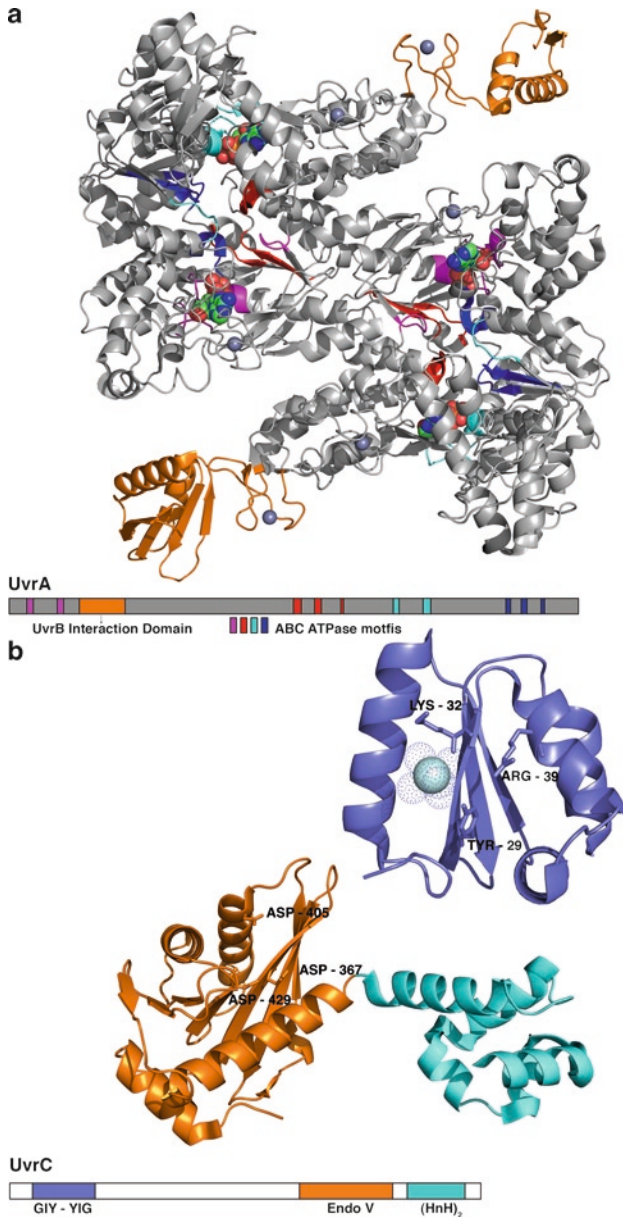


Fig. 3 Structural and functional motifs of bacterial NER proteins. **(a)** The UvrA dimer structure (PDB ID 2R6F): The UvrB-binding domain is shown in *orange*. For the first nucleotide-binding domain (NBDI), the Walker A and Q loop are shown in *magenta*; the Walker B, H loop, and signature sequence are shown in *red*. For the NBDII, the Walker A and Q loop are shown in *cyan*, the Walker B, H loop, and signature sequence are shown in *blue*. The Zn ions and ADP molecules are shown as CPK models. **(b)** The two distinct endonuclease centers of UvrC (PDB IDs: 1YD1, 2NRR): the N-terminal GIY-YIG family nuclease domain is shown in *blue*, and the residues that are essential for the cleavage are labeled. The metal and surrounding water molecules are shown as a CPK model. The C-terminal endonuclease domain is shown in *orange*, and the tandem HhH domain is shown in *cyan*. Residues that are necessary for the 5' incision are labeled. **(c)** The UvrB structure (PDB ID 2FDC): domain 1a is shown in *yellow*, 1b in *green*. Domain 2 is labeled as UvrA

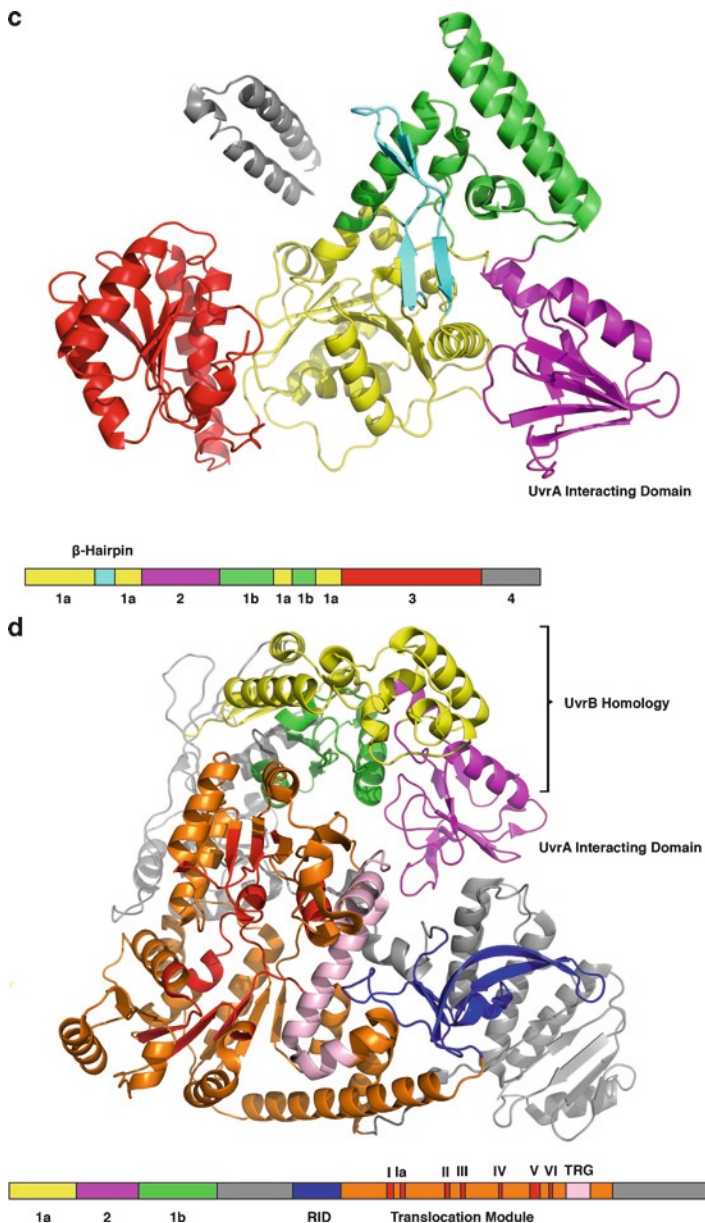


Fig. 3 (continued) interacting domain and shown in *magenta*. Domain 3 is shown in *red*, and a separate domain 4 peptide structure is shown in *grey*. The β hairpin motif in domain 2 is shown in *cyan*. UvrB belongs to the helicase superfamily II with six helicase motifs in domain 1a and domain 3. **(d)** The Mfd structure (PDB ID 2EYQ): The domains that are homologous to UvrB are shown in the same color scheme as for the UvrB molecule (1a in *yellow*, 2 in *magenta*, and 1b in *green*), and domain 2 is labeled as UvrA interacting domain. The translocation domain of Mfd, which is shown in *orange*, contains all seven SF2 helicase motifs which are shown in *red*. The RNAP interacting domain is shown in *blue*, and the TRG motif in *light pink*. Below the structure, the sequence of each protein is indicated and color-coded as in its respective structure

UvrA specifically recognizes a wide variety of DNA lesions by bending the DNA by approximately 55° (Peng et al. 2011) and unwinding the DNA by as much as 3 bp per binding event (Oh and Grossman 1986). The equilibrium dissociation constant (K_d) of *E. coli* UvrA for undamaged DNA was measured as 3–14 μ M, whereas the K_d for damaged DNA is much lower at 7–14 nM (Van Houten et al. 1987). Although binding of UvrA to the damaged DNA is specific and tight, it is also salt-sensitive and short-lived compared to the subsequently formed UvrB–DNA complex (Mazur and Grossman 1991).

2.2 The Central Player: UvrB

UvrB is a central player in NER because it interacts with all other NER components: UvrA, UvrC, UvrD, DNA polymerase I, and DNA. Several UvrB structures have been solved in the apo form (protein without ligand) (PDB ID: 1D9X, 1D2M, 1C4O, and 1T5L) in complex with ATP (PDB ID: 1D9Z) and in complex with DNA (PDB ID: 2FDC) (Machius et al. 1999; Theis et al. 1999; Truglio et al. 2004, 2006). The molecular weight of UvrB is ~75 kDa, and it is composed of five domains: 1a, 1b, 2, 3, and 4 (Theis et al. 2000), Fig. 3c. UvrB belongs to the helicase superfamily II. UvrB domains 1a and 3 are structurally related to the core domain of other helicases, and all the residues necessary to couple ATP hydrolysis to strand translocation are present within these two domains. The ATP-binding site is located at the interface of domains 1a and 3; a β -hairpin extends from domain 1a, and its tip interacts with domain 1b and forms a clamp for DNA binding; domain 2 is essential for UvrA interaction, and domain 4 is involved in both UvrA and UvrC interactions (Truglio et al. 2006). The C-terminal domain 4, which is linked to domain 3 by a flexible linker, was not observed in the original crystal structures; however, its structure (1E52) has been solved as a separate fragment (Alexandrovich et al. 1999; Sohi et al. 2000). Domain 4 adopts a helix–loop–helix fold and can form a dimer through specific hydrophobic and salt bridge interactions between residues in the loop region of this domain.

UvrB is a cryptic ATPase that can only be activated upon interaction with UvrA and damaged DNA, or when its autoinhibitory domain 4 is removed (Wang et al. 2006a). Unlike other helicases, UvrB exhibits a very limited DNA-unwinding ability (Gordienko and Rupp 1997). This activity was, therefore, described as “strand destabilization” rather than helicase activity and may function to merely distort the DNA at the lesion (Skorvaga et al. 2004). UvrB forms a complex with UvrA to verify the presence of the damaged nucleotide. The dsDNA is opened up by the insertion of UvrB’s β -hairpin between the two strands around the damaged site (Skorvaga et al. 2004). If no damaged DNA is present, UvrB promotes the dissociation of the UvrA–UvrB complex from the DNA. This “damage proofreading” ability of UvrB greatly increases the specificity of the NER process. If, however, the presence of the damage is verified, UvrA dissociates from the complex, and a stable UvrB–DNA preincision complex is formed.

The preincision UvrB–DNA complex is very stable with a dissociating reaction rate (k_{off}) of over 2 h. A padlock model, first proposed after the structural analysis of UvrB apoprotein, explains this remarkable slow off-rate at the atomic level: UvrB's flexible β -hairpin inserts itself between the two strands of the DNA and clamps one of the strands between the β -hairpin and domain 1b (Theis et al. 1999). Mutagenesis analysis added further support for this model and suggested that the highly conserved aromatic residues at the base of the hairpin are involved in the contact to the DNA (Skorvaga et al. 2004). Further validation of this model arose from a β -hairpin deletion ($\Delta\beta\text{h}$) study, in which the $\Delta\beta\text{h}$ UvrB mutant cannot form the preincision complex and thus cannot complete the UvrABC-mediated incision (Skorvaga et al. 2002). The crystal structure of a UvrB–DNA complex (PDB ID: 2FDC) has confirmed the padlock model and has demonstrated that one DNA strand threads behind the β -hairpin and that the nucleotide directly behind the β -hairpin is flipped out and inserted into a small highly conserved pocket of the protein (Truglio et al. 2006), see Figures 4 and 6a.

2.3 UvrC Mediates 3' and 5' Incision

The molecular weight of UvrC in multiple bacterial species is approximately 65 kDa, and it contains a potential UvrB-binding domain, two distinct endonuclease domains, and a tandem helix–hairpin–helix (HhH) DNA-binding domain. UvrC is responsible for both 3' and 5' incisions (Verhoeven et al. 2000). The preincision UvrB–DNA complex binds UvrC via the C-terminal domain of UvrB, domain 4. Deletion of this domain abolishes the UvrABC-mediated incision (Hsu et al. 1995). The structure of domain 4 adopts a helix–loop–helix conformation, in which two domain 4 molecules interact head-to-head through hydrophobic and ionic interactions (Alexandrovich et al. 2001). A region comprised of residues 205–239 in *E. coli* UvrC shares sequence homology with UvrB's domain 4, and the residues involved in the head-to-head hydrophobic and ionic interactions are well conserved in both proteins. With this sequence similarity in mind, this region of UvrC is predicted to be the UvrB-interacting domain and to share a similar structural fold and contacts as observed in the dimer of domain 4 from UvrB (Sohi et al. 2000).

Approximately 100 residues at the N-terminus of UvrC are responsible for the 3' cleavage, which occurs at the fourth or fifth phosphodiester bond 3' to the damaged site (Fig. 3b). This N-terminal domain (PDB ID: 1YD1) (Truglio et al. 2005) shares structural similarity to a GIY-YIG homing endonuclease. The structure of the N-terminal domain from *Thermotoga maritima* UvrC reveals that one divalent cation is present in the active site, which is coordinated by a glutamate and five coordinating water molecules arranged in an octahedral shape (Fig. 3b) (Truglio et al. 2005).

The structure of the C-terminal half of UvrC reveals that it contains two domains: a second endonuclease domain and a DNA-binding domain (PDB ID: 2NRR) (Karakas et al. 2007). The endonuclease domain is responsible for the incision at the eighth phosphodiester bond 5' to the damaged site. Although the endonuclease domain does not share sequence homology with any other known protein, its structure demonstrates a similar fold to the RNase H family (Karakas et al. 2007).

Interestingly, the helix–hairpin–helix (HhH) domain is connected to the endonuclease domain by a flexible linker, and it was proposed that it adopts a defined orientation relative to the endonuclease domain to orient the DNA toward the active site of the endonuclease domain. The isolated DNA-binding domain of *E. coli* UvrC prefers to bind to a bubble DNA substrate with at least six unpaired bases, which presumably mimics the structure of the DNA in the UvrB–DNA preincision complex. The structure of the DNA-binding domain (PDB ID: 1KFT) reveals that it consists of two HhH motifs, a motif which usually interacts with the phosphate backbone for non-specific DNA binding. The tandem HhH motif is essential for 5' incision, but not for 3' incision, except for lesions that exist in certain sequence contexts (Verhoeven et al. 2002). A similar fold is also found in the C-terminal domain of ERCC1, which forms a heterodimer with XPF, and is responsible for the 5' incision in human NER.

In some bacteria including *E. coli*, there is an UvrC homolog (Cho), which is upregulated in response to the SOS signal. Cho is homologous to the N-terminal half of UvrC and can incise the DNA several nucleotides further away on the 3' side of the lesion. This allows 3' incision of some unusually large lesions that would normally sterically block the access of UvrC to the incision site (Moolenaar et al. 2002; Van Houten et al. 2002).

2.4 Resynthesis and Ligation

UvrD, also known as helicase II, was one of the first enzymes to be characterized as a DNA helicase (Hickson et al. 1983). UvrD is involved in NER, mismatch repair, and recombination repair, as well as replication (Lahue et al. 1989). It is able to unwind duplex DNA 3'–5' at both nicked DNA substrates and blunt ends (Runyon et al. 1990). To recover UvrC from the incision complex (which contains UvrB, UvrC, and the incised DNA), UvrD is recruited by UvrB to the 3' incision site of the incised strand via protein–protein interactions (Ahn 2000) and unwinds the cleaved portion of the damaged DNA in a 3'–5' direction, causing UvrC to dissociate (Ahn 2000). Recently, it has been shown that UvrA and UvrB can together stimulate UvrD helicase activity (Atkinson et al. 2009). As UvrD (PDB ID: 2IS2) removes the damaged strand, it is believed that UvrB remains bound to the gapped DNA until the gap is filled by DNA polymerase I (Pol I). The resulting nick that is created by DNA polymerase I is joined by DNA ligase. As the final step of NER, DNA ligase catalyzes the phosphodiester bond formation (Tomkinson et al. 2006) (Fig. 4).

Fig. 4 (continued) nick and completes the repair patch. All the protein structures are shown in cartoon model except for the UvrB–DNA complex, which is shown in a space-filling model. The B-form of DNA was generated by the 3D-DART server (van Dijk and Bonvin 2009). The UvrA₂B₂ complex was created from three individual structures of UvrB (PDB ID: 2FDC), UvrA (PDB ID: 2R6F), and the contact interface of UvrA and UvrB (PDB ID: 3FPN). The UvrB–DNA complex was modified from the UvrB–DNA cocrystal structure (PDB ID: 2FDC). The other complexes were shown only for functional demonstration, and the location and orientation are not based on real structures

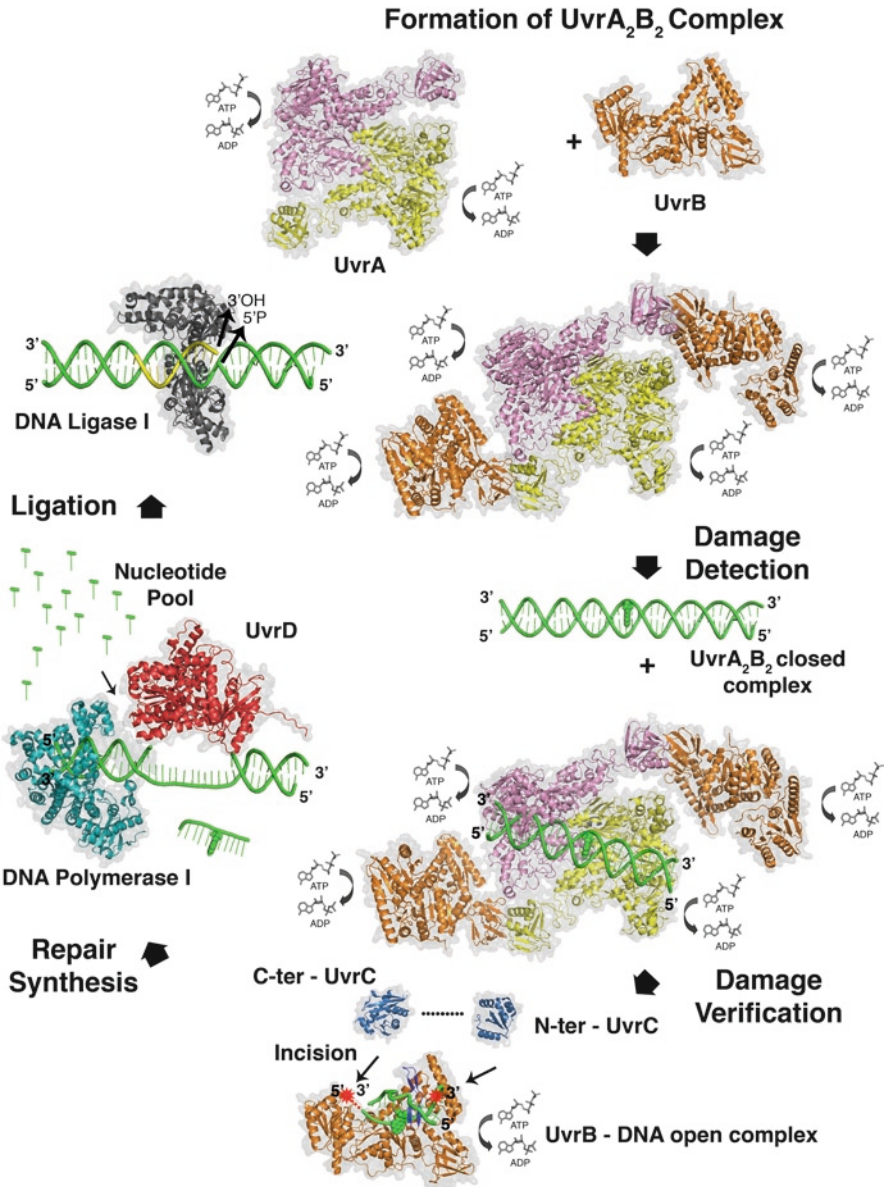


Fig. 4 Molecular model of prokaryotic NER. The dimeric UvrA protein (PDB ID: 2R6F) hydrolyzes both ATP and GTP. It also forms a complex with UvrB (PDB ID: 2FDC) and activates the ATPase activity of UvrB. The UvrA₂B₂ complex (PDB ID for the contact interface: 3FPN) first searches for the distortion along the DNA caused by the lesion. Then, UvrA transfers the damaged DNA to UvrB. During damage verification, the β-hairpin of UvrB (shown in *turquoise*) inserts between the two strands of DNA and forms a stable pre-incision complex, which is believed to activate UvrB's ATPase. Binding and hydrolysis of ATP by UvrB is essential for recruitment of UvrC. The N-terminal endonuclease domain of UvrC (PDB ID: 1YCZ) initiates the cut 4–5 nucleotides 3' to the damaged site followed by the 5' cut by C-terminal endonuclease domain of UvrC (PDB ID: 2NRR) eight nucleotides away from the lesion. UvrD (PDB ID: 2IS1) unwinds the DNA and releases the oligonucleotide containing the lesion. Simultaneously, DNA polymerase I (PDB ID: 2HHQ) synthesizes the missing strand. Finally, DNA ligase I (PDB ID: 1DGS) seals the

2.5 Transcription-Coupled Repair: Mfd

In both eukaryotic and prokaryotic cells, DNA damage in actively transcribed genes is repaired more rapidly than in inactive regions of the genome (Hanawalt 1989). The conserved repair process targeting the template strand with the stalled RNA polymerase (RNAP) at the lesion position is called transcription-coupled repair (TCR). Under these circumstances, RNAP is a damage sensor (Fig. 2). Transcription and DNA repair are coupled by a specific protein, which was named Mfd for *Mutation frequency decline*, a phenomenon first described in the 1970s. The structure of *E. coli* Mfd was solved in 2006 (Deaconescu et al. 2006) (PDB ID: 2EYQ). Mfd is a 130 kDa monomeric protein containing a potential UvrA-binding domain, a RNAP-interacting domain, and a translocation domain containing seven SF2 helicase motifs and one TRG (translocase in RecG) motif. The Mfd protein is able to release RNA polymerase (RNAP) stalled by a lesion on the template strand in an ATP-dependent manner (Selby and Sancar 1994). It is also able to recruit UvrA and stimulate the NER process (Selby and Sancar 1993) (Fig. 3d). The primary sequence and the three-dimensional structure of the N-terminal portion of Mfd is similar to UvrB domains 1a, 1b, and 2 (PDB ID: 2EYQ) (Selby and Sancar 1993; Deaconescu et al. 2006; Murphy et al. 2009). Since domain 2 of UvrB is the UvrA-binding domain, the corresponding region of Mfd is also expected to bind UvrA. Interestingly, Mfd lacks a motif like UvrB's β -hairpin for damage verification. Thus, Mfd may serve more as a platform to recruit the NER machinery rather than as a damage sensor or verifier. Further analysis of the putative UvrA-binding interface of Mfd shows that it is mostly buried and is not available for UvrA interaction. This suggests that in the absence of interacting with RNAP, Mfd is not capable of binding to UvrA. The interaction of Mfd with RNAP must, therefore, trigger a conformational change in Mfd, exposing the UvrA-binding site for UvrA binding (Murphy et al. 2009). After recruiting UvrA to the transcriptional stalled position by Mfd, TCR shares the same subsequent steps as global genome repair mentioned above.

3 NER in Eukaryotic Cells

3.1 Introduction

Proteins involved in eukaryotic NER are conserved from yeast to human (Table 2). NER in eukaryotes is very similar to prokaryotic NER in terms of the overall biochemical steps (damage recognition, verification, dual incisions, excision, repair synthesis, and ligation). However, what takes only six proteins in prokaryotes is carried out in eukaryotic cells by a total of 11 factors composed of more than 30 proteins. Therefore, the eukaryotic NER process depends on the intricate networks of protein-protein interactions that are important for the sequential binding, assembly, and correct positioning of the NER proteins on DNA (Gillet and Schärer 2006).

Table 2 Human and yeast NER proteins

Human Protein	Human		Yeast			Function
	AA	MW (kDa)	Protein	AA	MW (kDa)	
Cyclin H	323	38	CCL1	393	45	Kinase subunit of TFIIH
Cdk 7	346	39	KIN28	306	35	Kinase subunit of TFIIH
CSA (ERCC8)	396	44	RAD28	515	57	Interaction with Cockayne Syndrome type B (CSB) protein
CSB (ERCC6)	1493	168	RAD26	1085	125	A member of the SWI2/ SNF2 family of ATP- dependent chromatin remodeling factors, Transcription couple repair
CTEN2	172	20	CDC31	161	18	Interaction with XPC causing conformational changes
DDB1	1140	127				DDB subunit, with CUL4-RBX1 forms a E3 platform and interacts with various WD repeats protein
DDB2 (XPE)	427	48	PRP4	465	52	DDB subunit, defective in XPE
ERCC1	323	36	RAD10	210	24	Binding partner of XPF
FBL3 (FBXL2)	423	47	RAD7	565	64	With RAD16 forms E3 ubiquitin ligase and damage binding
p62 (GTF2H1)	548	62	TFB1	642	73	TFIIH subunit
p44 (GTF2H2)	395	44	SSL1			TFIIH subunit
p34 (GTF2H3)	308	34	TFB4	338	37	TFIIH subunit
p52 (GTF2H4)	462	52	TFB2	513	59	TFIIH subunit
TTDA (GTF2H5)	71	8	TFB5	72	8	TFIIH subunit
LIG1	919	102	CDC9	755	84	DNA ligase
MMS19L (MMS19)	1030	113	MET18	1032	118	Required for transcription and NER
MT1	309	36	TFB3			TFIIH subunit
			RAD16	790	91	With RAD7 forms E3 ubiquitin ligase and damage binding
HR23A	363	40	RAD23	398	42	RAD23B paralog
HR23B	409	43	RAD23	398	42	Forms complex with XPC
RPA1	616	68	RFA1	621	73	RPA subunit, binds ssDNA intermediates
RPA2	270	30	RFA2	273	30	Interaction with ssDNA intermediates

(continued)

Table 2 (continued)

Human Protein	Human		Yeast			Function
	AA	MW (kDa)	Protein	AA	MW (kDa)	
RPA3	121	14				Interaction with ssDNA intermediates
XAB2	1140	127	SYF1	859	100	Interaction with XPA
XPA	273	31	RAD14	1100	126	Interaction with DNA and proteins of the preincision complex
XPB (ERCC3)	782	89	SSL2	843	95	3'-to-5' DNA helicase TFIIH subunit
XPC	940	106	RAD4	754	87	Initial DNA damage recognition
XPB (ERCC2)	760	87	RAD3	778	90	5'-to-3' DNA helicase TFIIH subunit
XPF (ERCC4)	916	107	RAD1	1100	126	5' incision nuclease
XPG (ERCC5)	1186	133	RAD2	273	30	3' incision nuclease

In addition, eukaryotic NER is highly regulated at more complex levels, including transcription activation, posttranslational modifications, protein–protein interactions, protein degradation through ubiquitination, and chromatin remodeling (Araujo and Wood 1999; Sancar and Reardon 2004; Sugawara 2010). Similar to prokaryotic systems, eukaryotes also contain two NER subpathways: global genome repair (GGR) and transcription-coupled repair (TCR) (see section 1). GGR and TCR differ in the DNA damage recognition step. In human GGR, initial DNA damage recognition is carried out by the XPC–hHR23B complex and in some cases by the coordinated action of damaged DNA-binding protein 1 and 2 (DDB1 and DDB2) (Sugawara 2009) (Fig. 5).

In human TCR, initial DNA damage detection is achieved by the stalling of the RNA polymerase at the damaged site and subsequent tighter association with the Cockayne Syndrome B protein (CSB) (Hanawalt and Spivak 2008). For both GGR and TCR, all subsequent steps of the repair process are shared by both subpathways. After initial damage recognition, the ten-subunit containing transcription factor, TFIIH, is recruited to the damage and unwinds the DNA duplex around the lesion followed by recruitment of XPA, replication protein A (RPA), XPG, and finally the ERCC1–XPF complex (Schaeffer et al. 1993; Evans et al. 1997). An oligonucleotide of ~24–32 nt including the lesion is excised by the endonucleases ERCC1–XPF and XPG, which incise the DNA 5' and 3' relative to the lesion, respectively (O'Donovan et al. 1994). In contrast to the prokaryotic system, the 5' incision by ERCC1–XPF precedes the 3' incision by XPG (Staresinic et al. 2009). The dual incision reaction can be reconstituted using six factors on naked DNA or minichromosomes: XPC–hHR23B, TFIIH, XPA, RPA, XPF–ERCC1, and XPG. (Araki et al. 2000). Gap-filling synthesis is carried out by the coordinated action of DNA polymerase δ or ϵ and under certain cellular conditions also polymerase κ , proliferating cell nuclear antigen (PCNA), and replication factor C (RF-C). Finally, ligase I or XRCC1–DNA ligase III α (XRCC1–Lig3) seals the newly synthesized

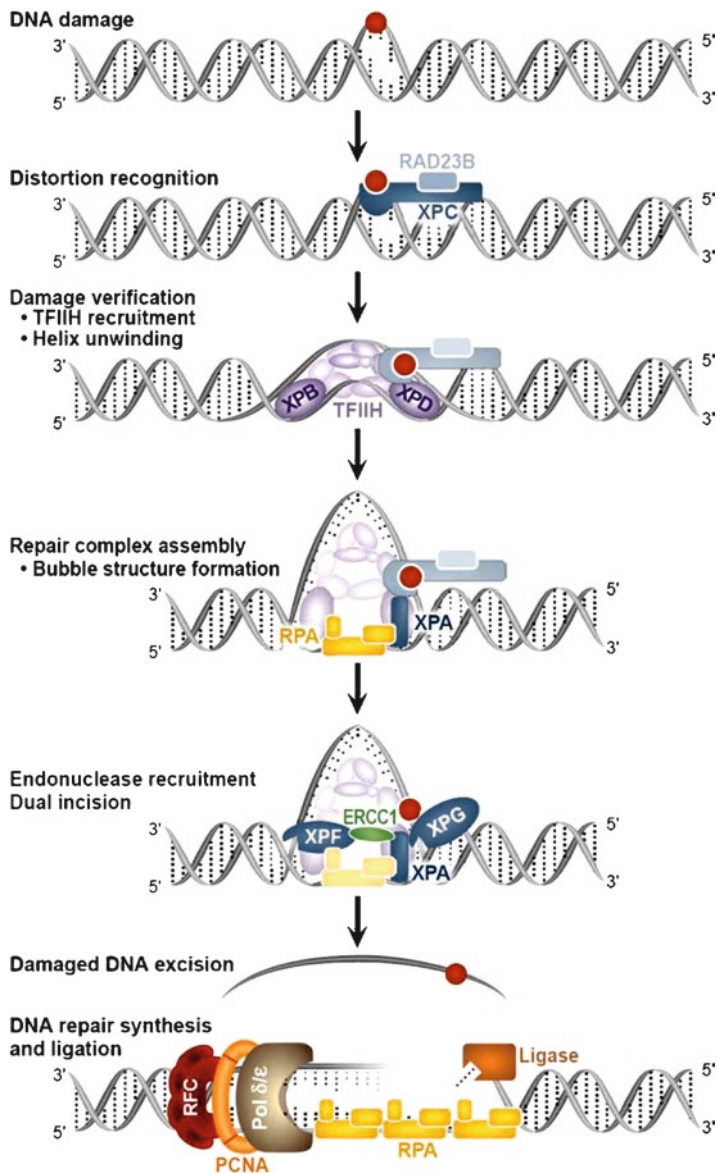


Fig. 5 Model of mammalian global genome repair. The mammalian NER process depends on the intricate networks of protein–protein interactions that are important for the sequential binding, assembly, and correct positioning of the NER proteins on DNA. See text for more details. UV-DDB is omitted from the diagram, and it is important to note that UV-DDB can facilitate the recognition of lesions that are poorly recognized by XPC such as UV-induced pyrimidine dimers. The diagram is adapted from the reference by Croteau et al. (2008)

repair patch to fully restore the integrity of the DNA (Moser et al. 2007). These reactions are summarized in Fig. 5.

Defects in the NER process can lead to one of several rare autosomal recessive diseases such as, xeroderma pigmentosum (XP), Cockayne syndrome (CS), and trichothiodystrophy (TTD), as well as others, which are shortly summarized at the end of this chapter. Seven NER-deficient genetic complementary groups for XP (XP-A to G), two for CS (CS-A and CS-B), and one for TTD (TTD-A) have been identified, and the responsible genes have been cloned.

3.2 Initial DNA Distortion Recognition: XPC–HR23 and UV-DDB

The XPC–HR23B, UV-DDB, XPA, RPA, and TFIIH proteins all play a role in DNA damage recognition. Accumulating evidence indicates that XPC–HR23B and UV-DDB are particularly important in the initial DNA distortion recognition in the GGR-NER pathway (Sugasawa et al. 2001; Volker et al. 2001). *In vivo*, XPC is tightly associated with one of the two mammalian homologues of the yeast Rad23 protein, most often with HR23B and less frequently with HR23A, both of which stabilize and stimulate XPC (Batty et al. 2000). Centrin 2/caltractin 1 (CEN2), a ubiquitously expressed centrosomal protein, also stimulates XPC activity *in vitro* (Araki et al. 2001).

The XPC–HR23B complex has a higher affinity for UV-induced 6-4 photo-products (6-4PP) than for cyclobutane pyrimidine dimers (CPD) (Batty et al. 2000). It also binds to other DNA lesions including a cholesterol-modified base (Kusumoto et al. 2001). The partial crystal structure of the yeast XPC orthologue, Rad4 (lacking the N-terminal 100 and C-terminal 122 residues), with Rad23 bound to DNA containing a CPD adduct, provides insight to its damage recognition properties (PDB ID: 2QSG), Fig. 6b (Min and Pavletich 2007). Rad4 interacts with the DNA using several motifs. The TGD (transglutaminase-homology domain) and BHD1 (beta hairpin domain 1) bind to 11 bp of undamaged dsDNA, while BHD2 and BHD3 bind to 4 bp of DNA containing the CPD lesion. The structure also reveals that a β -hairpin inserts itself through the DNA duplex, causing two damaged bases to flip out of the double helix (Fig. 6b) as part of the damage recognition

Fig. 6 (continued) of a truncated Rad4 bound to a Rad23 fragment with DNA containing a CPD lesion (CPD structure is not shown in the structure). Insertion of a β -hairpin through the DNA duplex causes the two damaged base pairs to flip out of the double helix. (c) XPD (PDB ID: 2VSF). In a XPD-DNA model, motifs shown in *magenta* could play a role in DNA binding to the FeS cluster. (d) UV-DDB (PDB ID: 3EI1) binds to 6-4PP. The contacts with DNA are made through the DDB2 subunit. DDB2 uses a β -hairpin that binds from the minor groove of DNA and extrudes the 6-4PP into a shallow binding pocket in the major groove. (e) Hypothetical model of UvrA binding to DNA based on crystal structure of UvrA (PDB ID: 2R6F). Two C-terminal zinc-finger domains in UvrA are important for specific binding of UvrA to damaged DNA (Croteau et al. 2006). All structures are shown in cartoon models except that DNA lesions, which are shown in CPK model

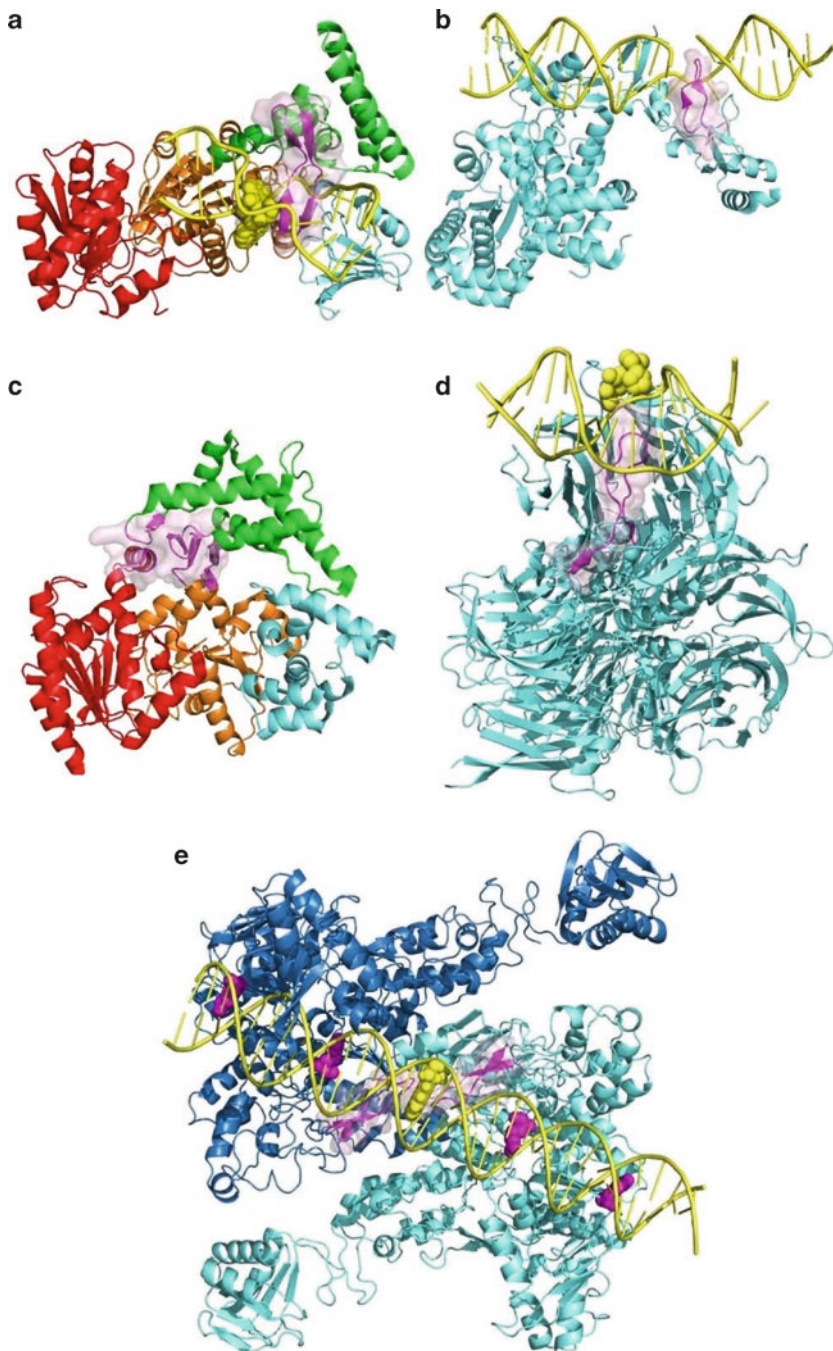


Fig. 6 DNA damage sensor motifs. DNA damage is recognized by similar motifs (in *magenta*) in different NER proteins. (a) DNA-binding model for UvrB based on the UvrB-DNA cocrystal structure (Jia et al. 2009). DNA was extended based on crystal structure and a BPDE was modeled into the DNA (PDB ID: 2FDC). The β -hairpin motif is inserted between two strands of DNA. The base directly behind the β -hairpin is flipped out and inserted into a small, highly conserved pocket in UvrB. (b) Rad4-Rad23-DNA structure (PDB ID: 2QSG). The crystal structure

mechanism. This β -hairpin motif is, thus, similar to the UvrB- β -hairpin motif involved in damage recognition (Fig. 6a). Interestingly, the crystal structure reveals that Rad4 does not interact directly with the damage; in fact, the CPD was disordered in the crystal structure, and the interactions with the DNA were restricted to the bases opposite to the damage and next to the damage.

Another important damage recognition factor in eukaryotic cells is UV-DDB, which can facilitate the recognition of lesions that XPC poorly recognizes such as UV-induced pyrimidine dimers (Fig. 1b). UV-DDB forms a complex with XPC (Sugasawa et al. 2005), and *in vitro* NER reactions are stimulated by the addition of UV-DDB with certain DNA lesions such as CPDs and 6-4PPs. UV-DDB consists of two subunits, p127 (or DDB1) and p48 (or DDB2 or XPE). XPE cells display a defect in GGR but have a normal TCR (Hwang et al. 1999). XPE cells exhibit ~50–80% UV-induced unscheduled DNA synthesis, indicating the presence of substantial GGR-NER activity (Keeney et al. 1994; Rasic Otrin et al. 1998). This is consistent with the observation that UV-DDB is dispensable in a cell-free system (Araujo et al. 2000). Purified DDB1-DDB2 has the highest affinity and specificity for 6-4PP, and it binds to CPDs, abasic sites, cis-diamminedichloroplatinum(II), 2–3 bp mismatches, and other chemical-induced lesions. UV-DDB arrives at UV-induced lesions prior to XPC recruitment and facilitates the recruitment of XPC–HR23 to both types of UV-induced lesions (6-4PPs and CPDs) *in vivo* (Rasic-Otrin et al. 2002).

A better understanding of UV-DDB damage recognition has been achieved by the crystal structures of UV-DDB (human DDB1-zebrafish DDB2) in complex with DNA containing 6-4PP or the abasic site analog, tetrahydrofuran (THF) (PDB ID: 3EI1) (Scrima et al. 2008). In the structure, an evolutionarily conserved hairpin from DDB2 inserts into the minor groove of the DNA duplex, leading to the flipping out of the two damaged pyrimidine bases or the THF and a regular base adjacent to the THF (Fig. 6d). This hairpin is strikingly similar to the wedge found in the crystal structure of EndoV (Scharer and Campbell 2009) and is reminiscent of both β -hairpin motifs in UvrB and Rad4 (Fig. 6a, b). Together, these structures highlight the importance of hairpin insertion, DNA bending, and base flipping in DNA damage recognition (Fig. 6). Surprisingly, the structural analysis of Rad4 and UV-DDB suggests that both proteins would not be able to bind simultaneously to the same DNA lesion (Scharer and Campbell 2009). Thus, the damaged site must be passed from one recognition complex to the next. While the exact mechanism of how the “baton of damage” is handed from one damage recognition partner to the next is currently unknown, as described below, ubiquitination of these key proteins may provide a path for this smooth handoff.

UV-DDB is also essential for the regulation of several NER processes. The UV-induced accumulation of p53 activates DDB2 transcription, leading to higher levels of UV-DDB (Adimoolam and Ford 2003). UV-DDB interacts with cullin 4A (CUL4A) and ROC1 and forms a supercomplex (DDB1–CUL4A^{DDB2}) that has ubiquitin E3 ligase activity. After UV exposure, the E3 ligase localizes to the site of damage, ubiquitinates XPC, and autoubiquitinates DDB2 (Dantuma et al. 2009; Sugasawa 2009). It was proposed that ubiquitination plays an important role in the XPC–HR23B-dependent displacement of UV-DDB (DDB1–CUL4A^{DDB2}) tightly bound to a DNA lesion.

3.3 Strand Opening and TFIIH

XPC–HR23B plays an essential role in GGR-NER in recruiting the basic transcription factor IIIH (TFIIH) to the damaged DNA site (Yokoi et al. 2000). The carboxyl terminus of XPC was shown to be essential for TFIIH recruitment (Yokoi et al. 2000). In contrast, during TCR-NER, RNA polymerase II and/or CSB facilitate the recruitment of TFIIH to the stalled transcription site (Tantin 1998). TFIIH is a multifaceted machine consisting of ten subunits: a core containing the seven subunits XPB, XPD, p62, p52, p44, p34, and p8/TTD-A coupled to the cdk-activating kinase (CAK) composed of Cdk7, cyclin H, and MAT1. A 3D model of TFIIH based on electron microscopy studies suggests that it is a ring-like structure that has a hole large enough to accommodate dsDNA (Chang and Kornberg 2000; Schultz et al. 2000). TFIIH possesses three enzymatic activities: an ATP-dependent DNA helicase, a DNA-dependent ATPase, and a kinase with specificity for the carboxyl-terminal domain of RNA polymerase II. TFIIH contains two ATP-dependent helicases: XPB and XPD. XPB and XPD display a 3′–5′ and 5′–3′ polarity, respectively (Egly 2001). It was found that the opening of the dsDNA around the damage is driven by the ATPase activity of XPB in combination with the helicase activity of XPD, while the helicase activity of XPB is dispensable for NER (Coin et al. 2007). Mutations in helicase motifs III (T469A) and VI (Q638A) in XPB that inhibit XPB’s helicase activity actually preserve the NER function of TFIIH. On the other hand, the helicase activity of XPD is dispensable for the transcription reactions, but not for the repair process (Coin et al. 2007).

XPD is a structural homolog of the prokaryotic NER protein UvrB (Bienstock et al. 2003; Dubaele et al. 2003), and it is required for the damage verification step. Crystal structures of XPD from three different archaeal species have been solved (PDB IDs: 3CRV, 3CRW, 2VL7, and 2VSF) (Fan et al. 2008; Liu et al. 2008; Wolski et al. 2008). The structures revealed that two domains adopt a Rec-A-like fold found in the SF1 and SF2 family of helicases. Two additional domains complete the structure, a domain harboring a 4Fe4S cluster and a novel “arch domain” (Fig. 6c). The first RecA-like domain together with the 4Fe4S cluster domain and the arch domain adopt a ring-like structure, and it was suggested that ssDNA passes through the hole formed by the three domains. A narrow pocket that can only accommodate single-stranded DNA was identified in the wall of this central hole and was proposed to play a role in damage discrimination (Wolski et al. 2008). Importantly, the crystal structures provided the first insight toward the effects of point mutations in XPD that lead to three distinct phenotypes: cancer-prone xeroderma pigmentosum (XP), the aging disorder Cockayne syndrome (CS), or trichothiodystrophy (TTD) (See section 4). Human XPD mutations that give rise to xeroderma pigmentosum are conserved in archaeal proteins and are clustered in the helicase motifs. These mutations lead to inactivation of XPD by impairing its ability to bind and hydrolyze ATP and thereby drastically reducing the helicase activity. Patients with a combination of XP and CS phenotypes suffer from a classical XP phenotype along with the severe neurological and developmental

abnormalities of CS (Lehmann 2003). Mutations generating the XP/CS phenotype are clustered around the ATP-binding site and are predicted to either produce or prevent important conformational changes. TTD mutants are mostly distributed within the helicase domains and are expected to cause framework defects impacting TFIIH integrity (Fan et al. 2008). Two additional mutations leading to TTD are found in the 4Fe4S cluster domain and in the arch domain, respectively, and are predicted to cause framework defects as well. Besides its helicase function, XPD also plays an architectural role by anchoring the CAK subcomplex to the core of TFIIH (Drapkin et al. 1996; Reardon et al. 1996).

3.4 Role of XPA-RPA

Two proteins that play important roles in damage verification are XPA and RPA. XPA was the first human NER protein that was demonstrated to have specificity for damaged DNA (Robins et al. 1991; Jones and Wood 1993). This 31-kDa protein interacts with DNA, as well as with several NER factors including RPA, TFIIH, and ERCC1. In the absence of XPA, no stable preincision complex can form, and no excision of damaged DNA occurs. Consequently, cells deficient in XPA are hypersensitive to UV radiation and chemical mutagens (Satokata et al. 1993). Single-stranded binding protein RPA also displays some preferential binding to damaged DNA (Clugston et al. 1992; He et al. 1995; Burns et al. 1996). The weak preference of XPA and RPA for damaged substrates is probably a function of their role as helix distortion recognition factors rather than their direct binding to the damaged nucleotide per se. This is reminiscent of how UvrA functions in prokaryotes. It was proposed that recruitment of XPA to the damaged site is an essential checkpoint during NER and can accelerate, under the appropriate situation, the removal of the damaged DNA by dissociating CAK from the core TFIIH (Coin et al. 2008).

3.5 5' and 3' Cleavage: XPF-ERCC1 and XPG

After TFIIH is recruited by XPC-HR23B to the damaged site, the DNA is unwound by approximately 20 bp. XPG prefers to bind to the unwound DNA, and it also interacts with TFIIH and XPA (Hohl et al. 2003). The stable binding of XPG to the unwound DNA triggers the release of the XPC-HR23B complex from the preincision complex, perhaps thereby adding an additional layer of specificity to the damage recognition process (Reardon and Sancar 2003). XPG contains two nuclease motifs, an N- and an I-domain separated by a large insertion, which interacts with TFIIH and contributes to substrate specificity (Dunand-Sauthier et al. 2005). The conserved N- and I-nuclease domains of XPG share homology to FEN1, which participates in base excision repair (Hohl et al. 2007). The incision made by XPG is 4–8 nucleotides 3' to the lesion, and it is independent from the 5'-incision made

by XPF–ERCC1 (Gillet and Schärer 2006). XPF–ERCC1 is a heterodimeric protein and is unstable when it is separated into monomers. XPF contains an N-terminal helicase-like domain, a nuclease domain, and a C-terminal tandem helix–hairpin–helix (HhH₂) domain (PDB ID: 2BGW) (Newman et al. 2005). ERCC1 contains an inactive nuclease domain and a C-terminal HhH₂ domain (Gaillard and Wood 2001). The association of XPF and ERCC1 is mediated by hydrophobic interactions between the C-terminal HhH₂ domains in both proteins (PDB ID: 1Z00) (Tripsianes et al. 2005). XPA and RPA are responsible for the recruitment of the XPF–ERCC1 complex to the damaged site. XPG is also required, but not catalytically, for recruiting XPF–ERCC1 to the damaged site, and it has been suggested that XPG may trigger a structural change in the preincision complex for XPF–ERCC1 binding (Tapias et al. 2004). After XPF–ERCC1 joins the preincision complex, it incises the phosphodiester bond at the 5′ side 15–24 nucleotides away from the lesion. In order to avoid the generation of single-stranded DNA intermediates, which are recombinogenic and mutagenic, dual incision and resynthesis are tightly coordinated. Recently, a “cut-patch-cut-patch” model has been proposed in which ERCC1/XPF mediates the 5′ incision followed by limited DNA synthesis, until it triggers XPG endonuclease activity to stimulate the 3′ incision, which allows the repair synthesis to be completed (Staresincic et al. 2009).

3.6 *Resynthesis and Ligation*

The resynthesis and ligation steps in NER are accomplished by a similar mechanism used for DNA replication. The polymerase processivity factor (PCNA) (Shivji et al. 1992) and DNA polymerases are involved in resynthesis. During the process, RPA is required to protect the undamaged single-stranded DNA from degradation (Coverley et al. 1991). PCNA forms a ring structure around the helical DNA (Gulbis et al. 1996). In order to encircle the DNA and to load onto the 3′-OH group generated by the XPF–ERCC1 cleavage reaction, the closed ring of PCNA has to be temporarily opened. A clamp loader, replication factor C (RFC), is required in this reaction. RFC is a heteropentameric complex with one large (140 kDa) and four small subunits (36–40 kDa). The ATPase activity of RFC is required to load PCNA onto the DNA and to form a functional PCNA clamp. After being loaded onto the DNA, PCNA can freely slide along the DNA and stabilize the DNA polymerase to ensure processive replication (Bravo et al. 1987). DNA polymerase δ (Yuzhakov et al. 1999) or Pol ϵ (Shivji et al. 1995) and, in some special cases, Pol κ (Ogi and Lehmann 2006) are then recruited to synthesize the new DNA strand and at the same time to displace the damage-containing oligonucleotide and NER components (TFIIH, XPA, XPG, and XPF/ERCC1). After gap-filling has been completed, the newly synthesized DNA is sealed by DNA ligase, most likely DNA ligase I (Timson et al. 2000). Yet, XRCC1–DNA ligase III α (XRCC1-Lig3) is also found to be necessary to seal the NER-induced breaks in quiescent cells (Moser et al. 2007).

3.7 *Transcription-Coupled Repair: CSA and CSB*

As mentioned in prokaryotic NER, actively transcribed DNA is repaired faster than the nontranscribed regions (Mellon et al. 1987). Transcription-coupled repair (TCR) is a subpathway of NER that specifically removes DNA lesions that cause stalling of the transcriptional machinery (Mellon 2005). When transcription is stalled at a lesion, recognition factors mediate the translocation of RNA polymerase away from the DNA damage to allow NER to proceed (Fig. 7). In humans, CSA and CSB are two recognition factors specifically involved in TCR (Hanawalt 2002). TCR utilizes all the proteins needed for global genome repair (GGR) except for the proteins that are required for initial damage recognition such as UV-DDB and XPC–HR23B, suggesting that the difference between TCR and GGR is only limited to the damage recognition step. In mammalian cells, CSB, a member of the SWI/SNF family of ATP-dependent chromatin remodeling factors, may play a similar role as Mfd in prokaryotes, although the reaction is much more complex and may involve other factors. Human CSB contains 1,493 amino acids which harbors seven characteristic ATPase motifs together with an acidic domain, a glycine-rich domain, and two putative nuclear localization signal (NLS) sequences (Troelstra et al. 1992). It exhibits DNA-binding activity and is a DNA-dependent ATPase *in vitro*. The functional CSB is a homodimer, and the dimer interface is located within the central ATPase domain (Christiansen et al. 2005). When RNA polymerase II (RNAPII) is stalled by a lesion during elongation, CSB recruits TFIIH to initiate TCR (Tantin 1998). CSB is necessary to recruit CSA and the core NER components (TFIIH, XPG, XPA, and ERCC1/XPF) to the lesion site, and to facilitate the interaction of the CSA complex with other chromatin remodeling factors (Fousteri et al. 2006). TCR of the transcribed strand beyond the TFIIH release point requires both CSA and CSB. CSA contains 396 amino acids and belongs to the family of WD-40 repeat proteins. A predicted CSA structure suggests that the N-terminal three WD repeats of CSA are involved in the interactions with CSB and p44, a subunit of RNAPII (Zhou and Wang 2001). Like DDB2, CSA interacts with DDB1–CUL4A–ROC1 and forms the DDB1–CUL4A^{CSA} E3–ubiquitin ligase complex, which presumably targets CSB for degradation following UV irradiation of the cells (Groisman et al. 2003). However, the precise role of CSA and CSB in the process of TCR remains unclear. The fate of the stalled RNA polymerase II is thought to be either being ubiquitinated in a CSA- and CSB-dependent manner (Bregman et al. 1996), or translocation away from the lesion without dissociation from the template strand (Hanawalt 2007). Recently, several groups have also suggested that RNAPII may remain at the damaged site during TCR (Laine and Egly 2006) (Fig. 7).

3.8 *NER and Chromatin Remodeling*

Inside living eukaryotic cells, DNA repair is carried out on chromosomes, which consist of linear DNA folded into several higher-order structures (Woodcock 2006). Chromatin structure and dynamics play important roles in DNA repair processes

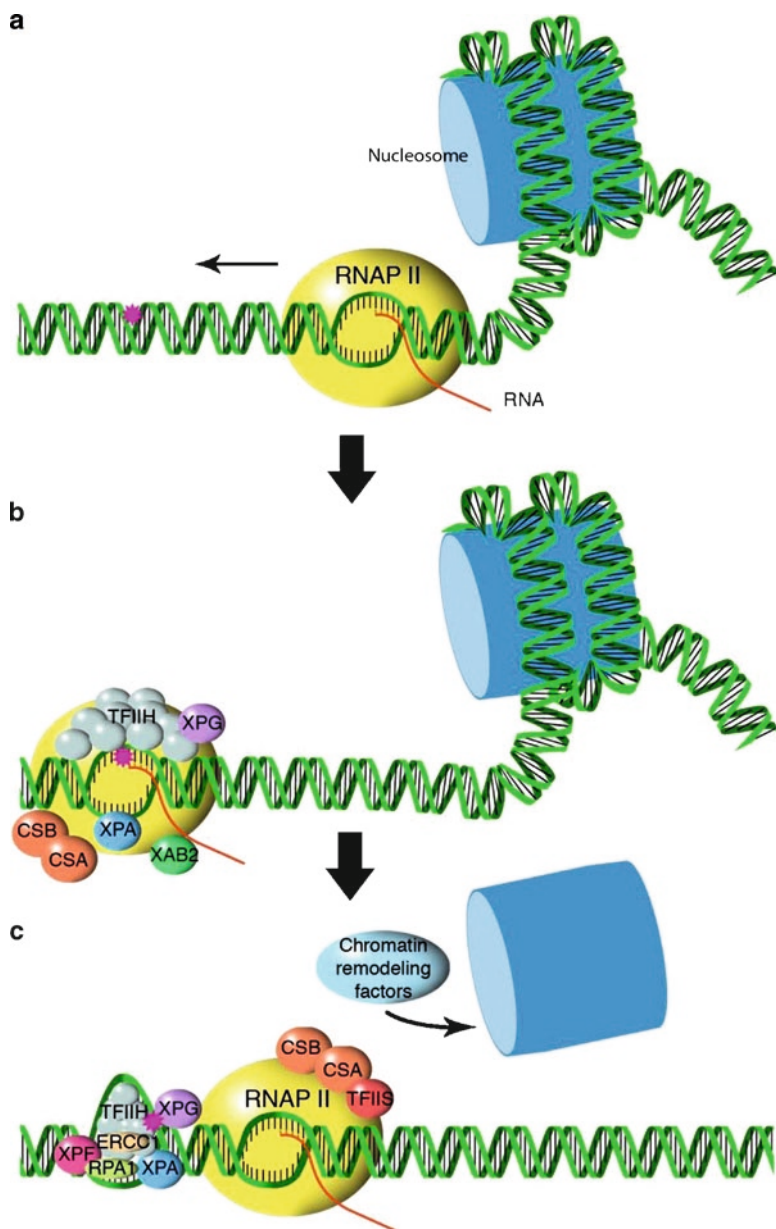


Fig. 7 Transcription-coupled repair in human cells and chromatin remodeling. (a) RNA polymerase (RNAPII in yellow) is shown being stalled at a damaged site. (b) This stalled complex recruits TFIIH (gray), XPG (purple), XPA (blue), XAB2 (green) and CSA and CSB (orange). (c) Through the action of TFIIS, CSA, and CSB, RNAP II backs away from the damaged site allowing access by the DNA repair machinery. Chromatin remodeling factors (light blue) are essential to remove nucleosomes from the damaged site and to allow movement of RNAPII and access by the DNA repair machine

(Nag and Smerdon 2009). Pioneering studies in the 1970s demonstrated that DNA damage in chromatin is refractory to DNA repair. The first report of chromatin remodeling during and after NER came from Smerdon and Lieberman (1978). These studies and several later studies led to the proposed “access, repair, and restore” model based on chromatin remodeling to explain the NER process within the complex chromatin environment (Smerdon 1991; Gong et al. 2005).

To overcome the inhibitory effect of chromatin, the first step prior to NER is the removal or remodeling of the chromatin to allow the access of repair proteins to the damaged DNA. This can be achieved through different mechanisms, which include posttranslational modification of histones, ATP-dependent modeling, and intrinsic dynamic changes, such as histone sliding and transient DNA unwrapping in nucleosomes (Osley et al. 2007).

Posttranslational modifications of histones includes acetylation, methylation, phosphorylation, poly(ADP)-ribosylation, and ubiquitylation of residues on both the histone “tails” and core regions (Turner 2002). In general, acetylation of lysine residues in core histones correlates with an open or more accessible chromatin structure. Several studies have demonstrated a relationship between hyperacetylation and enhanced damage recognition and NER repair (Ramanathan and Smerdon 1989; Brand et al. 2001). However, the exact role of histone acetylation during NER is still unclear. The extent and type of acetylation might vary for different DNA repair sites and NER pathways (GGR versus TCR) (Nag and Smerdon 2009).

Beside XPC and DDB2, additional substrates of the DDB1–CUL4A^{DDB2} E3 ligase complexes include histones H2A, H3, and H4 at UV-damaged DNA sites (Wang et al. 2006b). It has been shown that H3 and H4 ubiquitination makes the nucleosomes more accessible, and thus, ubiquitination of histones provides an additional mechanism for overcoming the inhibitory effect of chromatin on NER.

ATP-dependent remodeling factors use the energy derived from ATP hydrolysis to disrupt histone–DNA interactions, leading to nucleosome sliding, octamer transfer, or directional DNA translocation from the nucleosome (Osley et al. 2007). Furthermore, activity of the SWI/SNF remodeling complex is enhanced by the repair proteins XPA, XPC, and RPA (Hara and Sancar 2002), suggesting that NER proteins and remodeling factors may work synergistically to allow the access of repair proteins to damaged DNA. After completion of the NER process, the original chromatin structures need to be restored to maintain genetic and epigenetic information. Chromatin assembly factor 1 (CAF-1) has been shown to facilitate this process (Green and Almouzni 2003), Fig. 7.

4 NER and Human Disease

Earlier in this chapter, we learned that different mutations in one gene, XPD, a helicase subunit of TFIIH, can cause three different human pathologies: xeroderma pigmentosum, trichothiodystrophy, and Cockayne syndrome. Over the past 40 years, it has become clear that mutations of genes involved in TCR or GGR can lead to

serious autosomal recessive disorders with a broad spectrum of phenotypes including increased skin cancer, sun sensitivity, premature aging, and neurodegeneration. This section briefly summarizes a number of these syndromes.

Initially, mutations in the CSB gene were only associated with the disease Cockayne syndrome, but more recently, additional disorders have been identified such as the UV sensitivity syndrome (UV^SS), cerebro-oculo-facio-skeletal syndrome and the De Sanctis–Cacchione syndrome (DSC). Even though these disorders differ from each other, the underlying effects of these mutations are a sensitivity to UV radiation and the disability to complete transcription after UV radiation.

4.1 Cockayne Syndrome

The English pediatrician A. E. Cockayne first described the syndrome in 1936 in patients that presented with dwarfism, retinal atrophy, and deafness (Cockayne 1936). In 1992, after a review of 140 different cases, it became clear that there is a wide spectrum of symptoms in Cockayne patients and that the severity of the disease differs significantly, thus suggesting that there is considerable genetic heterogeneity among the patients (Nance and Berry 1992). The main hallmarks of Cockayne syndrome are severe growth retardation and progressive neurological dysfunction. In addition, the following symptoms can be observed: cutaneous photosensitivity, ocular abnormalities such as cataracts or progressive pigmentary retinopathy, sensorineural deafness, dental abnormalities, and cachectic dwarfism. Owing to the variability in symptoms, patients are now classified as having either the classical type I Cockayne syndrome (CS I) with a life expectancy into adolescence or young adulthood, or a particularly severe case classified as Cockayne syndrome II (CS II), which is characterized by an early onset of the disease and severe progression of the symptoms. The mean age of death within this second group is 6–7 years (Nance and Berry 1992). In contrast to xeroderma pigmentosum, however, the patients have no predisposition to cancer. Mutations leading to Cockayne syndrome are not limited to the *CSB* gene but have also been identified in the *CSA* gene (Rapin et al. 2000). CS can also arise from mutations in *XPD* or *XPG* genes (Cleaver et al. 2009).

4.2 Cerebro-Oculo-Facio-Skeletal Syndrome

Cerebro-oculo-facio-skeletal syndrome (COFS) is the most severe of the Cockayne syndrome like-diseases, and the mean age of death among the patients is only 3.5 years. For a clear diagnosis, the following criteria should be present: congenital microcephaly, ocular abnormalities, arthrogryposis, severe developmental delay, severe postnatal growth failure, and facial dysmorphism (Laugel et al. 2008). Intermediate

cases between CS I, CS II, and COFS suggest that the three diseases represent a continuous spectrum of severity (Laugel et al. 2008). COFS patients with mutations in either the *XPD* or *XPG* or *CSB* gene have been identified (Graham et al. 2001).

4.3 *De Sanctis–Cacchione Syndrome*

The De Sanctis–Cacchione syndrome was described in 1932 for the first time, and the symptoms include severe neurological and developmental degeneration, dwarfism, hypogonadism, and facial freckling (De Sanctis and Cacchione 1932; Reed et al. 1977). The disease is a subtype within the patients suffering from xeroderma pigmentosum (see Sect. 4.6). Some cases have been assigned to the CS-B complementation group (Itoh et al. 1996), but others have been identified in any of the XP complementation groups, so far mostly in the XP-A complementation group (Kanda et al. 1990).

4.4 *Trichothiodystrophy*

TTD, a rare autosomal syndrome of sulfur-deficient brittle hair, scaly skin, and mental and physical retardation, was first described by Davies and coworkers in 1968 (Pollitt et al. 1968). The patients also have abnormal facial appearance, and about 50% show increased sensitivity to sunlight (Cleaver et al. 2009). The most severe cases of TTD are caused by mutations in *XPD* or *XPB*, which as described above are subunits of TFIIH. Mutations in the small 8-kDa stabilizing factor, *GTF2H5*, are also associated with TTD (Giglia-Mari et al. 2004; Ranish et al. 2004). While these patients show increased sensitivity to sunlight, they have not shown increased cases of skin cancer. This is in contrast to a mouse knock-in model containing a human mutation in the *TTD* gene, which shows that high fluencies of UV can induce skin tumors (Cleaver et al. 2009).

4.5 *UV Sensitivity Syndrome*

In 1994 Itoh et al. described the UV sensitivity syndrome, which was observed in two Japanese siblings. The cells of these patients are three- to fourfold more sensitive to UV radiation and exhibit mild skin abnormalities. The disease, however, is very mild, and the patients have no defects in growth, mental development, and life expectancy. On the cellular level, UV^S cells and CS cells react in a similar way to UV radiation with an increased sensitivity to the cytotoxic effects of UV-induced damage, reduced recovery of RNA synthesis but normal levels of GGR (Itoh et al. 1994). Interestingly, in two patients, the mutation in the *CSB* gene results in a severely truncated protein,

and the presence of the CSB protein was not detectable, suggesting that the total absence of the protein can be less severe than the mutated protein. Recent findings, however, have suggested that these patients could develop CS-like symptoms later in life (Hashimoto et al. 2008). A clear difference between CS and UV^SS cells is the absence of increased sensitivity to oxidative stress in UV^SS cells, which may explain the differences in the pathological phenotypes of CS and UV^SS (Nardo et al. 2009).

4.6 Xeroderma Pigmentosum

This syndrome was first recognized in 1870 by two dermatologists, Ritter and Kaposi, who observed that the patients had “parchment skin” xeroderma. Later, the word “pigmentosum” was added to indicate the remarkable hyper and hypopigmentations, which occurred on sun-exposed areas. Patients with XP show severe sensitivity to sunlight and a ~2,000-fold increase in basal and squamous carcinomas, with the average onset of skin cancer being at age eight. In the late 1960s, Cleaver connected the disease with a deficiency in NER. Complementation analysis indicated that there were seven genetic loci, XPA-G that can give rise to XP. An eighth complementation group, XP variant (XPV) encodes a translesion DNA polymerase eta, which inserts AA opposite to a TT cyclobutane dimer; mutations that inactivate this polymerase cause a different polymerase to bypass the dimer, causing increased sunlight-induced mutations. Besides the extraordinary sensitivity to sunlight, a large portion of the patients (XPA, XPB, XPD, and XPG) also show neurodegeneration (Cleaver et al. 2009). It has been hypothesized that certain forms of oxidative DNA damage such as cyclo-dA or cyclo-dG, which are repaired by NER, might accumulate in XP patients and cause cell death and loss of critical neurons (Brooks et al. 2000).

Acknowledgments We apologize to all our colleagues working in this field for any omissions or lack of citations due to space limitations. We thank Drs. Vesna Ropic-Ortrin, Li Lan, and Satoshi Nakajima along with Amy Furda at Hillman Cancer Institute, University of Pittsburgh Medical Center for helpful suggestions and comments. This work was supported by UPCI-startup and NIH grant, 1R01ES019566-01 (BVH), the Deutsche Forschungsgemeinschaft (KI-562/2-1 and Forschungszentrum FZ-82) (CK) and K99ES016758-01 (HW). A new structure of a UvrA-DNA complex was recently published, and is very similar to the predicted structure shown in Figure 6e; Nowak, J.M. et al, (2011) *Nat. Struct. Mol. Biol.* 2:191–7.

References

- Adimoolam, S. and Ford, J. M. (2003). *DNA Repair (Amst)* 2: 947–54.
- Ahn, B. (2000). *Mol Cells* 10: 592–7.
- Alexandrovich, A., Sanderson, M. R., et al. (1999). *FEBS Lett* 451: 181–5.
- Alexandrovich, A., Czisch, M., et al. (2001). *J Biomol Struct Dyn* 19: 219–36.
- Araki, M., Masutani, C., et al. (2000). *Mutat Res* 459: 147–60.

- Araki, M., Masutani, C., *et al.* (2001). *J Biol Chem* 276: 18665–72.
- Araujo, S. J. and Wood, R. D. (1999). *Mutat Res* 435: 23–33.
- Araujo, S., Tirode, J. F., *et al.* (2000). *Genes Dev* 14: 349–59.
- Atkinson, J., Guy, C. P., *et al.* (2009). *J Biol Chem* 284: 9612–23.
- Batty, D., Rapic'Otrin, V., *et al.* (2000). *J Mol Biol* 300: 275–90.
- Bienstock, R. J., Skorvaga, M., *et al.* (2003). *J Biol Chem* 278: 5309–16.
- Boyce, R. P. and Howard-Flanders, P. (1964). *Proc Natl Acad Sci USA* 51: 293–300.
- Brand, M., Moggs, J. G., *et al.* (2001). *EMBO J* 20: 3187–96.
- Bravo, R., Frank, R., *et al.* (1987). *Nature* 326(6112): 515–7.
- Bregman, D. B., Halaban, R., *et al.* (1996). *Proc Natl Acad Sci USA* 93: 11586–90.
- Brooks, P. J., Wise, D. S., *et al.* (2000). *J Biol Chem* 275: 22355–62.
- Burns, J. L., Guzder, S. N., *et al.* (1996). *J Biol Chem* 271: 11607–10.
- Caron, P. R., Kushner, S. R., *et al.* (1985). *Proc Natl Acad Sci USA* 82: 4925–9.
- Chang, W. H. and Kornberg, R. D. (2000). *Cell* 102: 609–13.
- Christiansen, M., Thorslund, T., *et al.* (2005). *FEBS J* 272: 4306–14.
- Cleaver, J. E., Lam, E. T., *et al.* (2009). *Nat Rev Genet* 10: 756–68.
- Clugston, C. K., McLaughlin, K., *et al.* (1992). *Cancer Res* 52: 6375–9.
- Cockayne, A. E. (1936). *Arch Dis Child* 11: 1–8.
- Coin, F., Oksenysh, V., *et al.* (2007). *Mol Cell* 26: 245–56.
- Coin, F., Oksenysh, V., *et al.* (2008). *Mol Cell* 31: 9–20.
- Coverley, D., Kenny, M. K., *et al.* (1991). *Nature* 349: 538–41.
- Croteau, D. L., DellaVecchia, M. J., *et al.* (2006). *J Biol Chem* 281: 26370–81.
- Croteau, D. L., Peng, Y., *et al.* (2008). *DNA Repair* 7: 819–26.
- Dantuma, N. P., Heinen, C., *et al.* (2009). *DNA Repair (Amst)* 8: 449–60.
- Deaconescu, A. M., Chambers, A. L., *et al.* (2006). *Cell* 124: 507–20.
- DellaVecchia, M. J., Croteau, D. L., *et al.* (2004). *J Biol Chem* 279: 45245–56.
- De Sanctis, C. and Cacchione, A. (1932). *Riv Sper Freniatr Med Leg Alienazioni Ment* 56: 269–292.
- Doolittle, R. F., Johnson, M. S., *et al.* (1986). *Nature* 323: 451–3.
- Drapkin, R., Le Roy, G., *et al.* (1996). *Proc Natl Acad Sci USA* 93: 6488–93.
- Dubaele, S., Proietti De Santis, L., *et al.* (2003). *Mol Cell* 11: 1635–46.
- Dunand-Sauthier, I., Hohl, M., *et al.* (2005). *J Biol Chem* 280: 7030–7.
- Egly, J. M. (2001). *FEBS Lett* 498: 124–8.
- Evans, E., Moggs, J. G., *et al.* (1997). *EMBO J* 16: 6559–73.
- Fan, L., Fuss, J. O., *et al.* (2008). *Cell* 133: 789–800.
- Fousteri, M., Vermeulen, W., *et al.* (2006). *Mol Cell* 23: 471–82.
- Gaillard, P. H. and Wood, R. D. (2001). *Nucleic Acids Res* 29: 872–9.
- Giglia-Mari, G., and Coin, F., *et al.* (2004). *Nat Genet* 36: 714–9.
- Gillet, L. C. and Scharer, O. D. (2006). *Chem Rev* 106: 253–76.
- Gong, F., Kwon, Y., *et al.* (2005). *DNA Repair (Amst)* 4: 884–96.
- Gorbalenya, A. E. and Koonin, E. V. (1990). *J Mol Biol* 213: 583–91.
- Gordienko, I. and Rupp, W. D. (1997). *EMBO J* 16: 889–95.
- Graham, J. M., Jr., Anyane-Yeboah, K., *et al.* (2001). *Am J Hum Genet* 69: 291–300.
- Green, C. M. and Almouzni, G. (2003). *EMBO J* 22: 5163–74.
- Groisman, R., Polanowska, J., *et al.* (2003). *Cell* 113: 357–67.
- Gulbis, J. M., Kelman, Z., *et al.* (1996). *Cell* 87: 297–306.
- Hanawalt, P. C. (1989). *Genome* 31: 605–11.
- Hanawalt, P. C. (2002). *Oncogene* 21: 8949–56.
- Hanawalt, P. C. (2007). *Mol Cell* 28: 702–7.
- Hanawalt, P. C. and Haynes, R. H. (1965). *Biochem Biophys Res Commun* 19: 462–7.
- Hanawalt, P. C. and Spivak, G. (2008). *Nat Rev Mol Cell Biol* 9: 958–70.
- Hara, R. and Sancar, A. (2002). *Mol Cell Biol* 22: 6779–87.
- Hashimoto, S., Suga, T., *et al.* (2008). *J Invest Dermatol* 128: 1597–9.
- He, Z., Henricksen, L. A., *et al.* (1995). *Nature* 374: 566–9.

- Hickson, I. D., Arthur, H. M., *et al.* (1983). *Mol Gen Genet* 190: 265–70.
- Hill, R. F. (1958). *Biochim Biophys Acta* 30: 636–7.
- Hohl, M., Thorel, F., *et al.* (2003). *J Biol Chem* 278: 19500–8.
- Hohl, M., Dunand-Sauthier, I., *et al.* (2007). *Nucleic Acids Res* 35: 3053–63.
- Howard-Flanders, P., Boyce, R. P., *et al.* (1966). *Genetics* 53: 1119–36.
- Hsu, D. S., Kim, S. T., *et al.* (1995). *J Biol Chem* 270: 8319–27.
- Husain, I., Van Houten, B., *et al.* (1985). *Proc Natl Acad Sci USA* 82: 6774–8.
- Hwang, B. J., Ford, J. M., *et al.* (1999). *Proc Natl Acad Sci USA* 96: 424–8.
- Itoh, T., Ono, T., *et al.* (1994). *Mutat Res* 314: 233–48.
- Itoh, T., Cleaver, J. E., *et al.* (1996). *Hum Genet* 97: 176–9.
- Jia, L., Kropachev, K., *et al.* (2009). *Biochemistry* 48: 8948–57.
- Jones, C. J. and Wood, R. D. (1993). *Biochemistry* 32: 12096–104.
- Kanda, T., Oda, M., *et al.* (1990). *Brain* 113: 1025–44.
- Karakas, E., Truglio, J. J., *et al.* (2007). *EMBO J* 26: 613–22.
- Keeney, S., Eker, A. P., *et al.* (1994). *Proc Natl Acad Sci USA* 91: 4053–6.
- Kusumoto, R., Masutani, C., *et al.* (2001). *Mutat Res* 485: 219–27.
- Lahue, R. S., Au, K. G., *et al.* (1989). *Science* 245: 160–4.
- Laine, J. P. and Egly, J. M. (2006) *EMBO J* 25: 387–97.
- Laugel, V., Daloz, C., *et al.* (2008). *J Med Genet* 45: 564–71.
- Lehmann, A. R. (2003). *Biochimie* 85: 1101–11.
- Liu, H., Rudolf, J., *et al.* (2008). *Cell* 133: 801–12.
- Machius, M., Henry, L., *et al.* (1999). *Proc Natl Acad Sci USA* 96: 11717–22.
- Mazur, S. J. and Grossman, L. (1991). *Biochemistry* 30: 4432–43.
- Mellon, I. (2005). *Mutat Res* 577: 155–61.
- Mellon, I., Spivak, G., *et al.* (1987). *Cell* 51: 241–9.
- Min, J. H. and Pavletich, N. P. (2007). *Nature* 449: 570–5.
- Moolenaar, G. F., van Rossum-Fikkert, S., *et al.* (2002). *Proc Natl Acad Sci USA* 99: 1467–72.
- Moser, J., Kool, H., *et al.* (2007). *Mol Cell* 27: 311–23.
- Murphy, M. N., Gong, P., *et al.* (2009). *Nucleic Acids Res* 37: 6042–53.
- Myles, G. M. and Sancar, A. (1991). *Biochemistry* 30: 3834–40.
- Nag, R. and Smerdon, M. J. (2009). *Mutat Res* 682: 13–20.
- Nance, M. A. and Berry, S. A. (1992). *Am J Med Genet* 42: 68–84.
- Nardo, T., Oneda, R., *et al.* (2009). *Proc Natl Acad Sci USA* 106: 6209–14.
- Newman, M., Murray-Rust, J., *et al.* (2005). *EMBO J* 24: 895–905.
- O'Donovan, A., Davies, A. A., *et al.* (1994). *Nature* 371: 432–5.
- Ogi, T. and Lehmann, A. R. (2006). *Nat Cell Biol* 8: 640–2.
- Oh, E. Y. and Grossman, L. (1986). *Nucleic Acids Res* 14: 8557–71.
- Orren, D. K. and Sancar, A. (1990). *J Biol Chem* 265: 15796–803.
- Osley, M. A., Tsukuda, T., *et al.* (2007). *Mutat Res* 618: 65–80.
- Pakotitrapha, D., Inuzuka, Y., *et al.* (2008). *Mol Cell* 29: 122–33.
- Peng, Y., Ghodke, H., *et al.* (2011). Unpublished.
- Pollitt, R. J., Jenner, F. A., *et al.* (1968). *Arch Dis Child* 43: 211–6.
- Ramanathan, B. and Smerdon, M. J. (1989). *J Biol Chem* 264: 11026–34.
- Ranish, J. A., Hahn, S., *et al.* (2004). *Nat Genet* 36: 707–13.
- Rapic Otrin, V., Kuraoka, I., *et al.* (1998). *Mol Cell Biol* 18: 3182–90.
- Rapic-Otrin, V., McLenigan, M. P., *et al.* (2002). *Nucleic Acids Res* 30: 2588–98.
- Rapin, I., Lindenbaum, Y., *et al.* (2000). *Neurology* 55: 1442–9.
- Reardon, J. T. and Sancar, A. (2003). *Genes Dev* 17: 2539–51.
- Reardon, J. T., Ge, H., *et al.* (1996). *Proc Natl Acad Sci USA* 93: 6482–7.
- Reed, W. B., Sugarman, G. I., *et al.* (1977). *Arch Dermatol* 113: 1561–3.
- Robins, P., Jones, C. J., *et al.* (1991). *EMBO J* 10: 3913–21.
- Runyon, G. T., Bear, D. G., *et al.* (1990). *Proc Natl Acad Sci USA* 87: 6383–7.
- Sancar, A. and Reardon, J. T. (2004). *Adv Protein Chem* 69: 43–71.

- Sancar, A. and Rupp, W. D. (1983). *Cell* 33: 249–60.
- Setlow, I., Iwai, K., et al. (1993). *Gene* 136: 345–8.
- Schaeffer, L., Roy, R., et al. (1993). *Science* 260: 58–63.
- Scharer, O. D. and Campbell, A. J. (2009). *Nat Struct Mol Biol* 16: 102–4.
- Schultz, P., Fribourg, S., et al. (2000). *Cell* 102: 599–607.
- Scrima, A., Konickova, R., et al. (2008). *Cell* 135: 1213–23.
- Selby, C. P. and Sancar, A. (1993). *Science* 260: 53–8.
- Selby, C. P. and Sancar, A. (1994). *Microbiol Rev* 58: 317–29.
- Setlow, R. B. and Carrier, W. L. (1964). *Proc Natl Acad Sci USA* 51: 226–31.
- Shivji, K. K., Kenny, M. K., et al. (1992). *Cell* 69: 367–74.
- Shivji, M. K., Podust, V. N., et al. (1995). *Biochemistry* 34: 5011–7.
- Skorvaga, M., Theis, K., et al. (2002). *J. Biol Chem* 277: 1553–9.
- Skorvaga, M., DellaVecchia, M. J., et al. (2004). *J Biol Chem* 279: 51574–80.
- Smerdon, M. J. (1991). *Curr Opin Cell Biol* 3: 422–8.
- Smerdon, M. J. and Lieberman, M. W. (1978). *Proc Natl Acad Sci USA* 75: 4238–41.
- Sohi, M., Alexandrovich, A., et al. (2000). *FEBS Lett* 465: 161–4.
- Staresincic, L., Fagbemi, A. F., et al. (2009). *EMBO J* 28: 1111–20.
- Sugasawa, K. (2009). *DNA Repair (Amst)* 8: 969–72.
- Sugasawa, K. (2010). *Mutat Res* 685: 29–37.
- Sugasawa, K., Okamoto, T., et al. (2001). *Genes Dev* 15: 507–21.
- Sugasawa, K., Okuda, Y., et al. (2005). *Cell* 121: 387–400.
- Tantin, D. (1998). *J Biol Chem* 273: 27794–9.
- Tapias, A., Auriol, J., et al. (2004). *J Biol Chem* 279: 19074–83.
- Theis, K., Chen, P. J., et al. (1999). *EMBO J* 18: 6899–907.
- Theis, K., Skorvaga, M., et al. (2000). *Mutat Res* 460: 277–300.
- Timson, D. J., Singleton, M. R., et al. (2000). *Mutat Res* 460: 301–18.
- Tomkinson, A. E., Vijayakumar, S., et al. (2006). *Chem Rev* 106: 687–99.
- Tripsianes, K., Folkers, G., et al. (2005). *Structure* 13: 1849–58.
- Troelstra, C., van Gool, A., et al. (1992). *Cell* 71: 939–53.
- Truglio, J. J., Croteau, D. J., et al. (2004). *EMBO J* 23: 2498–509.
- Truglio, J. J., Rhau, B., et al. (2005). *EMBO J* 24: 885–94.
- Truglio, J. J., Karakas, E., et al. (2006). *Nat Struct Mol Biol* 13: 360–4.
- Turner, B. M. (2002). *Cell* 111: 285–91.
- van Dijk, M. and Bonvin, A. M. (2009). *Nucleic Acids Res* 37(Web Server Issue): W235–9.
- Van Houten, B. and Snowden, A. (1993). *Bioessays* 15: 51–9.
- Van Houten, B., Gamper, H., et al. (1987). *J Biol Chem* 262: 13180–7.
- Van Houten, B., Gamper, H., et al. (1988). *J Biol Chem* 263: 16553–60.
- Van Houten, B., Eisen, J. A., et al. (2002). *Proc Natl Acad Sci USA* 99: 2581–3.
- Verhoeven, E. E., van Kesteren, M., et al. (2000). *J Biol Chem* 275: 5120–3.
- Verhoeven, E. E., van Kesteren, M., et al. (2002). *Nucleic Acids Res* 30: 2492–500.
- Volker, M., Mone, M. J., et al. (2001). *Mol Cell* 8: 213–24.
- Wang, H., DellaVecchia, M. J., et al. (2006a). *J Biol Chem* 281: 15227–37.
- Wang, H., Zhai, L., et al. (2006b). *Mol Cell* 22: 383–94.
- Wolski, S. C., Kuper, J., et al. (2008). *PLoS Biol* 6: e149.
- Woodcock, C. L. (2006). *Curr Opin Struct Biol* 16: 213–20.
- Yokoi, M., Masutani, C., et al. (2000). *J Biol Chem* 275: 9870–5.
- Yuzhakov, A., Kelman, Z., et al. (1999). *EMBO J* 18: 6189–99.
- Zhou, H. X. and Wang, G. (2001). *Cell Biochem Biophys* 35: 35–47.